by mutual collisions or scattering into Charon or Pluto. Debris captured into some corotation islands could also have been dislodged through encounters with other high-eccentricity material. Nevertheless, it seems plausible that a fraction comparable to the tiny masses of P1 and P2 might have survived such stochastic removal processes.

What about corotation resonances other than the 4:1 and 6:1? For an eccentric Charon, the 3:1 corotation resonance is nearly overlapped by its Hill sphere at apocenter and was likely not a stable niche. Corotation resonances also occur when $(m + p)n \approx pn_C$ for $p > 1$, but these fall at distances $a_{cr} = (m/p + 1)^{2/3}$ and are shifted inward. Thus, those that fall in the vicinity of P1 and P2 have amplitudes that are dependent on a higher power of Charon's eccentricity (i.e., $\sim e_C^{3p}$, e_C^{5p}) and are weaker. Although transient forced eccentricities may interfere with the stability of adjacent $p = 1$ resonances, it remains an intriguing possibility that smaller, yet undetected moons may orbit Pluto near the 5:1.

Because the corotation resonances we invoke no longer exist, direct diagnostic evidence of this mechanism is elusive. However, a circumstantial case can be made by considering the alternatives. Although there are capture mechanisms (*4*, *5*) to create well-separated secondaries such as some Kuiper belt binaries, they do not select a common orbital plane or direction. In addition, the subsequent hardening of these configurations tends to produce large eccentricities that could not be damped by tidal forces given the small masses of P1 and P2 (*2*). Alternatively, if a protosatellite disk were to extend to sufficient distance to allow the accretion of P1 and P2 in situ, there is no obvious reason why they should be found in near-resonant orbits, because tidal torques are also too weak to migrate them into such configurations. A final unanswered question is how the moons were initially trapped in corotation resonances. One possibility is that a small amount of vapor and/or small particles extended past the location of the 6:1 resonance ($\sim 3.3\ a_C$) and their free eccentricities damped by collisional viscosity. This could have initially populated many resonance sites, but most would be later cleared as eccentricities were excited by resonant migration. Indeed, material comprising P1 and P2 may have begun as ring arcs, except that by lying external to Pluto's Roche limit, single moons were able to accumulate.

References and Notes

1. H. A. Weaver *et al.*, *Nature* **439**, 943 (2006).
2. S. A. Stern *et al.*, *Nature* **439**, 946 (2006).
3. M. W. Buie, W. M. Grundy, E. F. Young, L. A. Young, S. A. Stern, *Astron. J.* **132**, 290 (2006).
4. P. Goldreich, Y. Lithwick, R. Sari, *Nature* **420**, 643 (2002).
5. S. J. Weidenschilling, *Icarus* **160**, 212 (2002).
6. W. B. McKinnon, *Astrophys. J.* **344**, L41 (1989).
7. R. M. Canup, *Science* **307**, 546 (2005).
8. R. M. Canup, *Ann. Rev. Astron. Astrophys.* **42**, 441 (2004).
9. A. R. Dobrovolskis, S. J. Peale, A. W. Harris, in *Pluto and Charon*, S. A. Stern, D. J. Tholen, Eds. (Univ. Arizona Press, Tucson, AZ, 1997), pp. 193–219.
10. P. Goldreich, S. Tremaine, N. Borderies, *Astron. J.* **92**, 490 (1986).
11. F. Namouni, C. Porco, *Nature* **417**, 45 (2002).
12. C. D. Murray, S. F. Dermott, *Solar System Dynamics* (Cambridge Univ. Press, Cambridge, 2001).
13. S. Dermott, R. Malhotra, C. D. Murray, *Icarus* **76**, 295 (1988).
14. D. Brouwer, *Astron. J.* **68**, 152 (1963).
15. P. Goldreich, S. Tremaine, *Astrophys. J.* **243**, 1062 (1981).
16. Methods are available as supporting material on *Science* Online.
17. C. B. Olkin, L. H. Wasserman, O. G. Franz, *Icarus* **164**, 254 (2003).
18. The libration period is $2\pi/\omega_{lib} = T_{orb}(3e_C^m f_m(\alpha)\mu_C)^{-1/2}/(m + 1)$. With $e_C = 0.2$, the libration periods for the 4:1 and 6:1 are $\sim$11 and $\sim$112 times the local orbit periods, T_{orb}, respectively.
19. Because the tidal expansion rate (Eq. 7) decreases strongly as $a_C^{-11/2}$, the critical e_C value decreases with orbital radius as well, i.e., $e_{crit} \propto (R_p/a_{cr})^{5/m}$, so that the adiabatic constraint on e_C eases as Charon's orbit expands.
20. P. Goldreich, S. Soter, *Icarus* **5**, 375 (1966).
21. M. H. Lee, S. J. Peale, 2006. Preprint available at http://arxiv.org/abs/astro-ph/0603214.

22. This work was supported by NASA's Planetary Geology and Geophysics Program (W.R.W.) and NSF's Planetary Astronomy Program (R.M.C.). We thank S. A. Stern for communicating discovery results of Pluto's new moons just before publication and the referees for thoughtful comments.

Supporting Online Material

www.sciencemag.org/cgi/content/full/1127293/DC1
SOM Text

13 January 2006; accepted 23 June 2006
Published online 6 July 2006;
10.1126/science.1127293
Include this information when citing this paper.

Ice Record of $\delta^{13}C$ for Atmospheric CH_4 Across the Younger Dryas–Preboreal Transition

Hinrich Schaefer,[1,2*] Michael J. Whiticar,[1] Edward J. Brook,[2] Vasilii V. Petrenko,[3] Dominic F. Ferretti,[4,5] Jeffrey P. Severinghaus[3]

We report atmospheric methane carbon isotope ratios ($\delta^{13}CH_4$) from the Western Greenland ice margin spanning the Younger Dryas–to–Preboreal (YD-PB) transition. Over the recorded ~800 years, $\delta^{13}CH_4$ was around –46 per mil (‰); that is, ~1‰ higher than in the modern atmosphere and ~5.5‰ higher than would be expected from budgets without ^{13}C-rich anthropogenic emissions. This requires higher natural ^{13}C-rich emissions or stronger sink fractionation than conventionally assumed. Constant $\delta^{13}CH_4$ during the rise in methane concentration at the YD-PB transition is consistent with additional emissions from tropical wetlands, or aerobic plant CH_4 production, or with a multisource scenario. A marine clathrate source is unlikely.

Ice core records reveal prominent changes in atmospheric methane concentration [CH_4] associated with abrupt climate change (*1*) but the causes, including source and sink changes, remain controversial (*1*, *2*). Modern contributions from individual sources or sinks have been constrained by the $^{13}C/^{12}C$ ratio of atmospheric methane ($\delta^{13}CH_4$) (*3*, *4*). New analytical techniques extend this approach to air samples from gas occlusions in polar ice. Using ice samples from the Pakitsoq outcrop (Western Greenland) (*5*), we measured $\delta^{13}CH_4$ in air dating between 11,360 and 12,220 years before the present (yr B.P.) (*6*). The record covers the transition between the Younger Dryas (YD) and Preboreal Holocene (PB), when temperature (*7*) and [CH_4] (*1*) increased rapidly at the termination of the last ice age (Fig. 1).

The suitability of Pakitsoq ice for paleostudies has been demonstrated by the agreement of [CH_4] and other geochemical tracers with records from the Greenland Ice Sheet Project 2 (GISP2) ice core (*5*). Samples were collected during three field campaigns (2001 to 2003) by means of oil-free chainsaws and shipped frozen to the University of Victoria. The main data set was measured after wet extraction by gas chromatography–isotope ratio mass spectrometry (GC-IRMS) (*8*). [CH_4] measurements were duplicated at Washington State University. Six samples from three time periods were analyzed for $\delta^{13}CH_4$ at the National Institute of Water and Atmospheric Research (NIWA) using ~100-liter air samples extracted in the field (*8*) (Fig. 1). All samples were dated with a gas age scale derived by comparison of geochemical records from Pakitsoq and GISP2 (*8*). Results are consistent throughout the three field seasons and form a composite data set (Fig. 1).

[1]School of Earth and Ocean Sciences, University of Victoria, Post Office Box 3055, V8W 3P6, Canada. [2]Department of Geosciences, Oregon State University, 104 Wilkinson Hall, Corvallis, OR 97331, USA. [3]Scripps Institution of Oceanography, University of California, San Diego, Mail Code 0244, La Jolla, CA 92093, USA. [4]Institute of Arctic and Alpine Research, University of Colorado, Boulder, CO 80309, USA. [5]National Institute of Water and Atmospheric Research Limited, Post Office Box 14901, Wellington, New Zealand.

*To whom correspondence should be addressed. E-mail: schaefeh@geo.oregonstate.edu

Our $\delta^{13}CH_4$ data reveal several interesting features, two of which we discuss here. First, the YD-PB methane is ^{13}C-enriched by ~1 per mil (‰) relative to modern atmospheric $\delta^{13}CH_4$ (–47.1‰) (*9*) and ~5.5‰ higher than expected from previously proposed natural CH_4 budget scenarios (table S1) (*3*, *10*). Second, there is no significant change in $\delta^{13}CH_4$ across the YD-PB transition. In the Pakitsoq record, $[CH_4]$ rises from 490 to 750 parts per billion by volume (ppbv) at the transition, which is consistent with GISP2 data (*1*, *5*) (Fig. 1A). During the YD, $\delta^{13}CH_4$ has a mean of –46.0 ± 0.5‰ (1σ) (Fig. 1C). Slight variations fall within the envelope of uncertainty. The PB mean $\delta^{13}CH_4$ is –45.7 ± 1.2‰. Surprisingly, there is no significant difference in $\delta^{13}CH_4$ between the two climatic intervals, nor is there an isotope shift during the ~250-ppbv $[CH_4]$ increase.

Pre-anthropogenic $\delta^{13}CH_4$ was expected to be depleted in ^{13}C (relative to modern atmospheric CH_4) because of the absence of fossil fuel combustion, slash-and-burn agriculture, and landfills, all of which emit ^{13}C-enriched CH_4 (*3*). Such ^{13}C depletions are observed in ice from 100 to 300 yr B.P. (*11*–*13*), whereas 400 to 2000 yr B.P. values from the late preindustrial Holocene (LPIH) are unexpectedly ^{13}C-enriched, similar to our YD-PB $\delta^{13}CH_4$ (*12*).

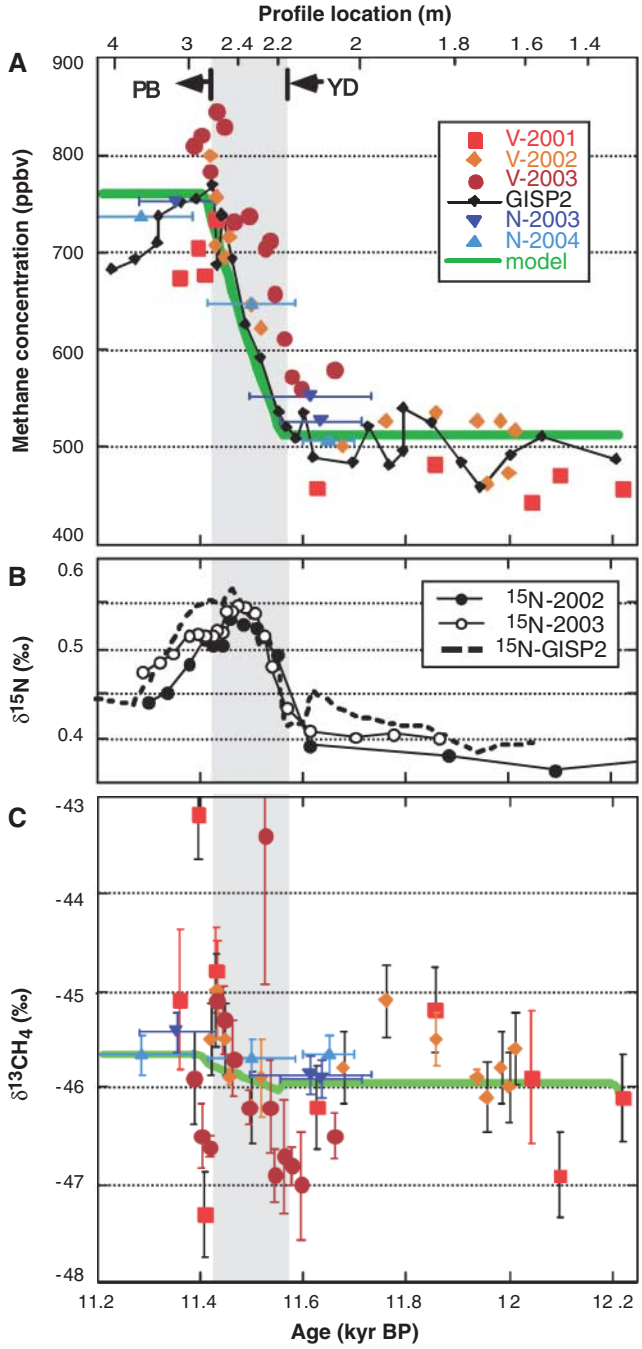

Fig. 1. Methane concentration and $\delta^{13}CH_4$ in Pakitsoq ice samples. **(A)** $[CH_4]$ measured at the University of Victoria (V-2001 to V-2003), at NIWA (N-2003 and N-2004), and from the GISP2 core, together with $[CH_4]$ model results used to constrain the transition source (*8*). The age spread of the samples is indicated by symbol size (V samples, 25 to 35 years) or horizontal bars (N samples, 100 to 240 years). The bottom axis shows sample age according to the Pakitsoq gas age scale (*8*); the top axis shows sample location within the profile (nonlinearity between the axes is due to differential thinning of ice layers). In (A) to (C), vertical shading marks the transition period. **(B)** Pakitsoq and GISP2 $\delta^{15}N$ data (*5*, *7*) show the onset of atmospheric warming (11,570 yr B.P.). **(C)** $\delta^{13}CH_4$ versus sample age. The slight depression of modeled $\delta^{13}CH_4$ (*8*) during the transition (~0.1‰) is due to a temporary imbalance between ^{13}C-depleted emissions and ^{13}C-enriching sinks (*22*). Data have been corrected for gravitational, thermal, and diffusion fractionation (*8*). Colored error bars show the standard error of multiple samples. Black error bars on single measurements show analytical precision (±1σ) derived from standard ice [0.44‰ (n = 11 replicates) in 2001, 0.37‰ (n = 33) in 2002, and 0.48‰ (n = 12) in 2003].

An initial explanation for our high $\delta^{13}CH_4$ was enrichment during postocclusion microbial oxidation of CH_4; that is, a storage artifact. However, this is ruled out because the amount of oxidation required for the observed isotopic shift would be between 15 and 48% (*8*). This would be readily detected as discrepancies between the Pakitsoq and GISP2 $[CH_4]$ records (Fig. 1A).

The difference between $\delta^{13}CH_4$ measured at the YD-PB and LPIH is not an artifact and must result from changes in CH_4 sources or sinks. The multitude of variables affecting atmospheric $\delta^{13}CH_4$ and uncertainties in paleoenvironmental data make it difficult to reconstruct a definitive CH_4 budget for the YD-PB. However, we discuss five possible explanations for the ^{13}C enrichment.

First, biomass burning is the most ^{13}C-enriched ($\delta^{13}CH_4$ ~ –25‰) of all sources (*3*). For the LPIH, elevated pyrogenic emissions of 25 Tg/year have been inferred from ice core $\delta^{13}CH_4$ (*12*). Even with fire emissions of this magnitude, the YD isotope scenario would still be too ^{13}C-depleted (table S1), whereas charcoal records indicate less burning before the LPIH (*14*). Nevertheless, literature estimates (*10*) of late glacial fire emissions (5 Tg/year) may be too low, and pyrogenic CH_4 could possibly contribute to ^{13}C enrichment. In the LPIH, high $\delta^{13}CH_4$ values have been partly attributed to human-made fires (*12*). Interestingly, we observe even higher $^{13}CH_4$ values in the YD-PB, when anthropogenic burning is expected to have been negligible.

Second, geologic (natural thermogenic) sources are usually not included in CH_4 budgets, even though they emit enough ^{13}C-enriched methane today to significantly affect atmospheric $\delta^{13}CH_4$ (*15*). Because of lower overall emissions during the YD, geologic sources probably constituted a larger fraction of the budget than today, leading to higher atmospheric $\delta^{13}CH_4$. Additionally, lower YD sea levels may have increased this source (*16*).

Third, previous CH_4 budget calculations have grouped tropical wetlands with other wetlands, resulting in integrated wetland $\delta^{13}CH_4$ of –58 to –59‰ (*3*, *4*). However, for tropical wetlands alone, flux-weighted mean $\delta^{13}CH_4$ as high as –53 to –55‰ has been reported (*17*). We suggest that tropical wetlands must be treated separately from boreal and temperate wetlands because of differences in climatic response and $\delta^{13}CH_4$. Tropical wetlands could partly account for the measured ^{13}C enrichment (table S1).

Fourth, the recent discovery of aerobic methane production (AMP) from plant material (*18*) has revealed a previously unknown source with high $\delta^{13}CH_4$ (~ –50‰). At estimated emission rates of 150 ± 90 Tg/year (*18*), it may be as important for the natural CH_4 cycle as wetlands (~140 Tg/year) (*19*) and could contribute to higher atmospheric $\delta^{13}CH_4$.

Fifth, there is evidence that Cl in the marine boundary layer (MBL) acts as a CH_4 sink, with a large isotope effect that increases atmospheric $\delta^{13}CH_4$ (*20*).

The potential impact of these five processes on $\delta^{13}CH_4$ can be estimated with isotope mass balance calculations. Although we recognize the considerable uncertainty introduced by the range of reported values and incomplete knowledge of YD conditions, we estimate that none of these processes alone can explain the ^{13}C enrichment. Conversely, the cumulative effect of all five would be too large (table S1). Several processes together could balance the YD isotope budget, but the exact combination cannot be determined without further evidence.

For completeness, one must also consider changes in the ratio of C_3 to C_4 vegetation, temperature-dependent fractionation coefficients, the relative amounts of CH_4 oxidation and production in wetland soils, and weighted total fractionation (α_{WT}) of the overall sink (*21*). These all influence atmospheric $\delta^{13}CH_4$, depending on climatic and anthropogenic factors that were probably different during the YD than today. Preliminary studies lead us to assume that neither the individual (±1‰), nor the combined impact of such changes (^{13}C depletion of 0.7‰), accounts for the $\delta^{13}CH_4$ enrichment.

A primary objective of our study is to understand why $[CH_4]$ increased abruptly during the YD termination. This rise was not associated with a sustained shift between steady states or with an episodic $\delta^{13}CH_4$ excursion (within measurement error) (Fig. 1). The latter observation suggests that the $[CH_4]$ increase was not caused by a short-lived perturbation, such as a release of stored CH_4.

Several lines of evidence suggest that increased emissions triggered by climate change caused the $[CH_4]$ rise (*1*, *2*). We used an atmospheric box model (*22*) to find the $\delta^{13}CH_4$ of these additional emissions or "transition source" required to explain our measured $[CH_4]$ and $\delta^{13}CH_4$ histories (*8*) (Fig. 1). Results depend on whether a MBL sink is considered and other uncertainties in α_{WT}. The model predicts a transition source $\delta^{13}CH_4$ between –53.6 ± 1.5‰ (including a MBL sink) and –50.7 ± 0.7‰ (without a MBL sink) (*23*).

The transition source could have been a combination of two or more sources. If those had different $\delta^{13}CH_4$ values, then their relative emissions would have to fortuitously match in order not to affect atmospheric $\delta^{13}CH_4$. For example, a ^{13}C-enriching component such as wildfire CH_4 or the marine Cl sink could be balanced by a ^{13}C-depleted microbial source. In the absence of unequivocal geologic evidence, these scenarios remain unresolved.

A sink decrease caused by higher volatile organic carbon emissions from forests (*24*) could have increased $[CH_4]$ without significant impact on α_{WT} and $\delta^{13}CH_4$. This scenario requires a large expansion of forests on the short time scale of the $[CH_4]$ increase. This may be compatible with paleobotanical data (*25*, *26*), but seems less likely when rates of ecosystem reorganization are considered. However, a slight sink decrease caused by feedbacks in atmospheric chemistry due to higher $[CH_4]$ is probable (*27*).

Most microbial CH_4 sources, such as boreal and temperate wetlands, animals, and clathrates, have $\delta^{13}CH_4$ of –60‰ or lower (*3*). The calculated impact of each of these sources on the transition mass balance would be –1.3 to –2.2‰ (depending on the assumed sink configuration). This exceeds the least significant difference of 1.1‰ between the YD and PB that would be discernible from our data at the 90% confidence level (based on a two-sided *t* test result of ±0.54‰). Therefore, microbial CH_4 can be ruled out as a sole transition source. However, CH_4 from marine clathrates can become ^{13}C enriched by microbial oxidation as it migrates through sediment and water columns (*28*). Isotopic fractionation associated with the oxidation progressively enriches the remaining CH_4 in ^{13}C relative to the clathrate. In order to match the transition source $\delta^{13}CH_4$, only 30 to 40% of the gas initially released from clathrates could have reached the atmosphere, according to the Rayleigh equation (*8*).

It has been proposed that marine clathrates drove the YD-PB $[CH_4]$ rise and maintained high $[CH_4]$ until mature wetlands developed (~8000 yr B.P.) (*2*). The total amount of clathrate dissociation required by this scenario can be calculated from (i) the magnitude of additional emissions (62×10^{12} g/year) (*1*), (ii) the fact that the latter represent only 30 to 40% of the destabilized clathrate gas, and (iii) the postulated time scale (~3000 years) (*2*), giving a result of 410×10^{15} to 540×10^{15} g of dissociated clathrate carbon. For comparison, only 175×10^{15} g potentially became unstable within the last 100,000-year glacial cycle (*29*), a period with more than 20 abrupt $[CH_4]$ rises (*1*). If clathrate release had driven all 20, then the potentially unstable reservoir for each event would have been exhausted within only ~50 years. In conclusion, our $\delta^{13}CH_4$ record supports neither catastrophic nor gradual clathrate emissions at the YD-PB transition, as is also indicated by CH_4 deuterium ($\delta D\text{-}CH_4$) records (*30*).

Hydrological proxies point to tropical wetlands as a driver of the YD-PB $[CH_4]$ increase (*31*, *32*). The higher of the $\delta^{13}CH_4$ values (–53 to –55‰) reported for tropical wetlands (*17*) closely matches the modeled transition source (especially if the MBL sink is included). The impact of tropical wetlands (0.1 to 0.7‰) on the mass balance during the transition would not be detectable. However, controversy remains about whether wetlands were a source of sufficient magnitude (*19*) and responded quickly enough to climate change (*2*).

In contrast, vegetation-derived AMP (*18*) could have changed quickly and strongly as indicated by paleoreconstructions of net primary productivity (NPP) (*33*). Scaling emission estimates (*18*) to NPP results in a potential increase of AMP by 50% between glacial and interglacial conditions. Terrestrial carbon stocks of vegetation, a possible proxy for AMP, reach equilibrium after climatic change within 250 years (*25*), and a first vegetation response occurs within decades (*26*). These time scales compare well with the observed lag time and duration of the YD-PB $[CH_4]$ increase (*7*). Also, the match between transition-source $\delta^{13}CH_4$ in the non-MBL sink scenario and that of AMP is good. In that case, the mass balance impact would be 0.7‰, which is within the uncertainty of our data. Whether the vegetation response was sufficient to sustain the $[CH_4]$ increase at the YD-PB should be investigated with vegetation models, once estimates of emission rates are confirmed. Our $\delta^{13}CH_4$ data are therefore consistent with a fast-responding AMP source and with the hypothesis that low-latitude wetlands caused $[CH_4]$ rises during the last glacial cycle (*1*).

Further insights into the atmospheric CH_4 budget require a reduction in the uncertainties of methane source and sink strengths and signals, and the combination of higher-precision $\delta^{13}CH_4$ and $\delta D\text{-}CH_4$ data.

References and Notes

1. E. J. Brook, S. Harder, J. Severinghaus, E. J. Steig, C. M. Sucher, *Global Biogeochem. Cycles* **14**, 559 (2000).
2. J. P. Kennett, K. G. Cannariato, I. L. Hendy, R. J. Behl, *Methane Hydrates in Quaternary Climate Change* (American Geophysical Union, Washington, DC, 2003).
3. M. J. Whiticar, in *Atmospheric Methane: Sources, Sinks and Role in Global Change*, M. A. K. Khalil, Ed. (NATO ASI Series, Springer, Berlin, 1993), vol. 113, pp. 138–167.
4. R. Hein, P. J. Crutzen, M. Heimann, *Global Biogeochem. Cycles* **11**, 43 (1997).
5. V. V. Petrenko, J. P. Severinghaus, E. J. Brook, N. Reeh, H. Schaefer, *Quat. Sci. Rev.* **25**, 865 (2006).
6. Years before the present are reported relative to 1950 A.D.
7. J. P. Severinghaus, T. Sowers, E. J. Brook, R. B. Alley, M. L. Bender, *Nature* **391**, 141 (1998).
8. Additional information on materials and methods is available on *Science* Online.
9. J. B. Miller *et al., J. Geophys. Res*. **107**, 10.1029/2001JD000630 (2002).
10. J. A. Chappellaz, I. Y. Fung, A. M. Thompson, *Tellus* **45B**, 228 (1993).
11. H. Craig, C. C. Chou, J. A. Welhan, C. M. Stevens, A. Engelkemeir, *Science* **242**, 1535 (1988).
12. D. F. Ferretti *et al.*, *Science* **309**, 1714 (2005).
13. T. Sowers *et al., Global Biogeochem. Cycles* **19**, 10.1029/2004GB002408 (2005).
14. C. Carcaillet *et al.*, *Chemosphere* **49**, 845 (2002).
15. G. Etiope, A. V. Milkov, *Environ. Geol.* **46**, 997 (2004).
16. B. Luyendyk, J. P. Kennett, J. F. Clark, *Marine Petrol. Geol.* **22**, 591 (2005).
17. P. D. Quay *et al.*, *Global Biogeochem. Cycles* **5**, 25 (1991).
18. F. Keppler, J. T. G. Hamilton, M. Braß, T. Röckmann, *Nature* **439**, 187 (2006).
19. J. O. Kaplan, *Geophys. Res. Lett*. **29**, 10.1029/2001GL013366 (2002).
20. W. Allan, D. C. Lowe, A. J. Gomez, H. Struthers, G. W. Brailsford, *J. Geophys. Res*. **110**, 10.1029/2004JD005650 (2005).

21. The MBL sink strongly affects α_{WT}. Accordingly, all reported sensitivity tests, including the ones on past changes in α_{WT} and transition isotope budgets, have been carried out with and without a MBL sink.
22. P. P. Tans, *Global Biogeochem. Cycles* **11**, 77 (1997).
23. α_{WT} without a MBL sink is taken as 6.4 ± 0.7‰, which is smaller than at present because of decreases in [Cl] (*34*) and soil uptake (*19*); including the MBL sink increases α_{WT} to 9.3 ± 0.7‰. All YD sinks were scaled proportionally to $[CH_4]$ from current estimates (*13*, *20*) to account for decreased loss rates at lower concentrations.
24. J. O. Kaplan, G. Folberth, D. A. Hauglustaine, *Global Biogeochem. Cycles* **20**, 10.1029/2005GB002590 (2006).
25. M. Scholze, W. Knorr, M. Heimann, *Holocene* **13**, 327 (2003).
26. D. Peteet, *Proc. Natl. Acad. Sci. U.S.A.* **97**, 1359 (2000).
27. A. M. Thompson, J. A. Chappellaz, I. Y. Fung, T. L. Kucsera, *Tellus* **45B**, 242 (1993).
28. N. J. Grant, M. J. Whiticar, *Global Biogeochem. Cycles* **16**, 10.1029/2001GB001851 (2002).
29. D. Archer, B. A. Buffett, *Geochem. Geophys. Geosyst.* **6**, Q03002 (2005).
30. T. A. Sowers, *Science* **311**, 838 (2006).
31. Y. J. Wang *et al.*, *Science* **294**, 2345 (2001).
32. K. A. Hughen, T. I. Eglinton, L. Xu, M. Makou, *Science* **304**, 1955 (2004).
33. L. M. Francois, C. Delire, P. Warnant, G. Munhoven, *Global Planet. Change* **16-17**, 37 (1998).
34. A. L. Rice, S. C. Tyler, M. C. McCarthy, K. A. Boering, E. Atlas, *J. Geophys. Res.* **108**, 10.1029/2002]D003042 (2003).
35. We thank N. Reeh and his team from the Technical University of Denmark for field collaboration and helpful discussions; P. Rose for field support; and P. Eby, L. Bjerkelund, P. Franz, K. Riedel, G. Brailsford, and R. Martin for laboratory assistance. Suggestions by two anonymous reviewers greatly improved this manuscript. The project was supported by a German Academic Exchange Service (DAAD) fellowship (H.S.), a Canadian Centre for Climate Modeling and Analysis Environment Canada grant (M.J.W.), a Natural Sciences and Engineering Research Council Discovery Grant (M.J.W.), Canadian Foundation for Climate and Atmospheric Sciences Project Grant GR-417 (M.J.W.), and NSF grants OPP-0221410 (E.J.B.) and OPP-0221470 (J.P.S.).

Supporting Online Material

www.sciencemag.org/cgi/content/full/313/5790/1109/DC1
Materials and Methods
Table S1
References

22 February 2006; accepted 14 July 2006
10.1126/science.1126562

Decoupled Plant and Insect Diversity After the End-Cretaceous Extinction

Peter Wilf,[1]* Conrad C. Labandeira,[2,3] Kirk R. Johnson,[4] Beth Ellis[4]

Food web recovery from mass extinction is poorly understood. We analyzed insect-feeding damage on 14,999 angiosperm leaves from 14 latest Cretaceous, Paleocene, and early Eocene sites in the western interior United States. Most Paleocene floras have low richness of plants and of insect damage. However, a low-diversity 64.4-million-year-old flora from southeastern Montana shows extremely high insect damage richness, especially of leaf mining, whereas an anomalously diverse 63.8-million-year-old flora from the Denver Basin shows little damage and virtually no specialized feeding. These findings reveal severely unbalanced food webs 1 to 2 million years after the end-Cretaceous extinction 65.5 million years ago.

There is little direct evidence from the fossil record about food web recovery after mass extinction. One theoretical model describes the rebuilding of diversity, after a lag period, first for primary producers and then for successively higher trophic levels after additional time lags (*1*). Consistent with this pattern is a 3- to 4-million-year recovery period for pelagic food webs after the Cretaceous-Paleogene boundary (K-T), inferred from isotopic depth gradients (*2*–*4*).

Insect damage on compressed fossil leaves provides abundant information about terrestrial food webs, because the diversity of plants and their insect feeding associations can be directly compared using the same fossils, at high sample sizes and in fine stratigraphic context (*5*–*7*). Modern ecological observations generally show positive correlations between insect herbivore diversity and plant diversity (*8*–*10*), and the evaluation of fossil insect damage can test whether past extinctions disrupted this linkage. In southwestern North Dakota, for example, the K-T event caused a significant floral extinction (*11*) accompanied by a major extirpation of insect feeding morphotypes (*6*). These included diverse and abundant leaf mines and galls, whose extant analogs are typically made by host-specialized insects (*12*, *13*). No significant recovery of specialized feeding was found in 80 m of local section representing the first ~0.8 million years of the 10-million-year Paleocene (*6*), prompting us to examine the geographic and temporal extent of the Paleocene ecological dead zone.

We investigated the recovery of plant-insect associations in the western interior United States, with emphasis on the Paleocene. We focused on insect mines (hereafter "mines") because they are a specialized feeding category commonly preserved in fine morphological detail (Fig. 1) (*14*, *15*). We compared four latest Cretaceous, nine early and late Paleocene, and one early Eocene megafloral sites (Table 1, table S1, and fig. S1) from warm temperate and subtropical fluvial paleoenvironments, selected to optimize preservation and diversity, sample size, stratigraphic control, and temporal and geographic coverage. The sites are located in several basins, forming a composite regional data set. Nearly all the Paleocene samples have similar taxonomic composition and the low floral diversity that is typical of the time period and region (Fig. 2 and tables S2 and S3). The major exception is the Castle Rock flora from the Denver Basin: a highly diverse and compositionally distinct early Paleocene assemblage with tropical rainforest characteristics, located in a warm and humid, apparently geographically restricted, belt on the eastern margin of the Laramide Front Range (*16*–*20*).

For taphonomic consistency, we analyzed only identifiable specimens of angiosperm leaves (excluding monocots) and avoided fragmentary leaves when possible. Samples came from single stratigraphic horizons whenever feasible, and biases were greatly reduced by either making quantitative census collections in the field (*7*) or using museum collections that had at least 400 identifiable specimens (Table 1). We also considered, where indicated below, more than 15,000 additional specimens that did not meet these criteria (table S4). These come from the North Dakota K-T study, Castle Rock, the late Paleocene and early Eocene of southwestern Wyoming, and one Late Cretaceous and two additional early Paleocene sites in the Denver Basin.

We scored each specimen for the presence or absence of 63 distinct insect damage morphotypes (DTs) found in the total data set, allocated to the four functional feeding groups of external foliage feeding, galling, mining, and piercing-and-sucking as described elsewhere (*5*, *14*, *15*) (table S2). Plant richness and DT diversity on bulk samples were standardized to 400 leaf specimens by means of rarefaction and randomized resampling, respectively (Fig. 2). Separately, we evaluated mining morphotype diversity for each of 89 species-site pairs with at least 25 leaf specimens (Fig. 3 and table S2).

The Cretaceous floras are rich, whereas all Paleocene assemblages are depauperate except Castle Rock (Fig. 2A), where plant diversity exceeds that of the Cretaceous samples. Insect damage diversity on bulk samples approximately tracks plant diversity, dropping across the K-T and remaining low until the latest Paleocene (Fig. 2 and table S4). However, insect damage shows a striking inversion with respect to plant richness at Castle Rock and Mexican Hat (Fig. 2). The diverse Castle Rock flora has some of the lowest feeding diversity in our data set. This result holds for all damage

[1]Department of Geosciences and Institutes of the Environment, Pennsylvania State University, University Park, PA 16802, USA. [2]Department of Paleobiology, Smithsonian Institution, Washington, DC 20560, USA. [3]Department of Entomology, University of Maryland, College Park, MD 20742, USA. [4]Department of Earth Sciences, Denver Museum of Nature and Science, Denver, CO 80205, USA.

*To whom correspondence should be addressed. E-mail: pwilf@psu.edu